2007 IEEE International Conference on
Robotics and Automation
Roma, Italy, 10-14 April 2007

Modeling and Identification of a 3 DOF Haptic Interface

A. Janot[1, 2], C. Bidard[1], F. Gosselin[1], M. Gautier[2], D. Keller[1], Y. Perrot[1]

[1] CEA/LIST
18 route du Panorama, BP 6, 92265 Fontenay aux Roses Cedex, France
[2] Institut de Recherche en Communication et en Cybernétique de Nantes
1, rue de la Noë - BP 92 101 - 44321 Nantes Cedex 03, France

Abstract— **The aim of haptic interfaces is to enhance the user's immersion in virtual environments through the stimulation of the haptic sense (motion capture and force feedback). Most devices make use of an articulated mechanical structure introducing distortions between the operator and the explored world. To assess the quality of the interface, this distortion must be identified. This paper deals with this issue and introduces the modeling and the identification of a 3 degrees of freedom haptic interface using inverse model and least squares method used in robotics.**

I. Introduction

An haptic interface is a force feedback device, which enables its user to interact with a virtual world or a remote environment explored by a slave device. It aims at the matching between the force and displacements given by the user and those applied to the virtual world.

Such systems are in growing demands for applications such as force feedback remote-control systems for extreme environment, man-machine interaction and training in professional operating procedures [1].

Usually, haptic interfaces make use of a mechanical actuated structure whose distal link is equipped with a handle. When manipulating this handle to interact with the explored world the user feels the apparent mass, compliance and friction of the interface. This distortion introduced between the operator and the virtual environment must be identified in order to enhance the design of the device and to develop appropriate control laws.

To do so, the system composed of the operator and the device is often modeled as a second order, sometimes with Coulomb friction, as in [2]-[4]. It has also been modeled as a series of second orders [5]. Several techniques of identification have been tested: in [6] the authors identify the device using spectral analysis while pulses are used in [5] to characterize another haptic device. In both cases, the distortion is locally identified relying on a specific model. Moreover, no statistical results such as deviations or relative deviations are given. Finally, dry friction is not considered in [6] while cable transmission is used. In [7], a parallel interface device is identified by means of relative least squares method and inverse model. However, the results are not given. In [8], a PHANToM™ was identified using the least squares method and the model given in [9]. However, the use of a Coulomb and viscous friction model is not well validated (therefore, specific tests of friction on the interfaces joints would have been necessary). Moreover, the conditioning number of the linear regressor is not considered. Consequently, it is impossible to know if the trajectories are enough exciting. Indeed, they used sinusoidal trajectories which generally do not excite well gravity and friction parameters. In [10]-[12], a parametric identification method adapted to multi DOFs systems, based on inverse model and least squares regression has been successfully applied to industrial robots. All these systems are stiff and have important inertias. It is interesting to check if it can also be applied to systems like haptic interfaces which exhibit a very different behavior. Indeed, they are very light, backdriveable and often used at low velocities. Hence, the compliance must be characterized and the model friction must be as accurate as possible. This means that additional identification tests must be designed compared to "classical" identification of industrial robots. First results obtained on a single DOF haptic interface using a cable transmission were encouraging [13]. Our purpose is to extend this result to multi-DOFs haptic devices. Therefore, we model and identify a three degrees of freedom haptic device.

The paper is organized as follows. The second and third sections present the general inverse dynamic model of a robot and the identification method. The 3 DOF haptic interface is presented in section 4. Its modeling and identification are detailed in sections 4 and 5. At last, the performances will be discussed in section 6.

II. General Inverse Dynamic Model

The inverse dynamic model (commonly called dynamic model) calculates the joint torques as a function of joint positions, velocities and accelerations. It is usually represented by the following equation:

$$\boldsymbol{\Gamma}=\mathbf{A(q)}\ddot{\mathbf{q}}+\mathbf{H(q,\dot{q})}+\mathbf{F_v}\dot{\mathbf{q}}+\mathbf{F_C}\,\mathbf{sign}(\dot{\mathbf{q}})+\mathbf{offset} \quad (1)$$

Where, $\boldsymbol{\Gamma}$ is the torques vector, $\mathbf{q}$, $\dot{\mathbf{q}}$ and $\ddot{\mathbf{q}}$ are respectively the joint positions, velocities and accelerations vector, $\mathbf{A(q)}$ is the inertia matrix, $\mathbf{H(q,\dot{q})}$ is the vector regrouping Coriolis, centrifugal and gravity torques, $\mathbf{F_v}$ and $\mathbf{F_C}$ are

Emails: alexandre.janot@cea.fr, maxime.gautier@irccyn.ec-nantes.fr, catherine.bidard@cea.fr, florian.gosselin@cea.fr

respectively the viscous and Coulomb friction matrices and offset is an offset torques vector.

The classical parameters used in this model are the components XX_j, XY_j, XZ_j, YY_j, YZ_j, ZZ_j of the inertia tensor of link j denoted ${}^j\mathbf{J}_j$, the mass of the link j called M_j, the first moments vector of link j around the origin of frame j denoted ${}^j\mathbf{MS}_j=[MX_j\ MY_j\ MZ_j]^T$, and the friction coefficients F_{Vj}, F_{Cj}. For the motorized joints, we add the actuator inertia called Iaj.

The kinetic and potential energies being linear with respect to the inertial parameters, so is the dynamic model [10]. It can thus be written as:

$$\mathbf{\Gamma}=\mathbf{D}(\mathbf{q},\dot{\mathbf{q}},\ddot{\mathbf{q}})\,\boldsymbol{\chi}_\mathbf{b} \quad (2)$$

Where $\mathbf{D}(\mathbf{q},\dot{\mathbf{q}},\ddot{\mathbf{q}})$ is a linear regressor and $\boldsymbol{\chi}_\mathbf{b}$ is a vector composed of the set of minimum inertial parameters.

The set of minimum inertial parameters represents the minimum number of parameters from which the dynamic model can be calculated. They can be deduced from the classical parameters by eliminating those which have no effect on the dynamic model and by regrouping some others. In fact, they represent the only identifiable parameters. In [10] a direct and recursive method of calculation of minimum parameters is described. It is efficient for robots having serial or tree structures. For closed loops, the minimum inertial parameters of the equivalent tree structure are a subset of those of the closed loops. Generally, additional relations from the constraint equations occur. These regroupings may be found using the QR decomposition numerical method [14] or dealing with the analytical equations. Some particular closed loop structures, as parallelogram, enable easier parameter regroupings [15].

III. Identification Method

Generally, ordinary least-squares (LS) technique is used to estimate the minimum inertial parameters solving an over-determined linear system obtained from a sampling of the dynamic model, along a given trajectory $(\mathbf{q},\dot{\mathbf{q}},\ddot{\mathbf{q}})$ [11], [12]. $\mathbf{X}$ being the b minimum parameters vector to be identified (same vector as $\boldsymbol{\chi}_\mathbf{b}$), $\mathbf{Y}$ the measurements vector (obtained by concatenation of the torques vector $\mathbf{\Gamma}$ over the whole trajectory), $\mathbf{W}$ the observation matrix (obtained by concatenation of the linear regressor over the whole trajectory) and $\boldsymbol{\rho}$ the vector of errors, the system is described as follows:

$$\mathbf{Y}=\mathbf{W}\mathbf{X}+\boldsymbol{\rho} \quad (3)$$

The L.S. solution $\hat{\mathbf{X}}$ minimizes the 2-norm of the vector of errors $\boldsymbol{\rho}$. $\mathbf{W}$ is a r×b full rank and well conditioned matrix, obtained by tracking exciting trajectories and by considering the minimum inertial parameters, r being the number of samplings along a trajectory. Hence, there is only one solution $\hat{\mathbf{X}}$ [12]. Standard deviations $\sigma_{\hat{X}_i}$ are estimated using classical and simple results from statistics. The matrix $\mathbf{W}$ is supposed deterministic, and $\boldsymbol{\rho}$, a zero-mean additive independent noise, with a standard deviation such as:

$$\mathbf{C}_{\rho\rho}=E(\rho^T\rho)=\sigma_\rho^2\,\mathbf{I}_\mathbf{r} \quad (4)$$

where E is the expectation operator and $\mathbf{I}_\mathbf{r}$, the r×r identity matrix. An unbiased estimation of σ_ρ is:

$$\hat{\sigma}_\rho^2=\|\mathbf{Y}-\mathbf{W}\hat{\mathbf{X}}\|/(r-b) \quad (5)$$

The covariance matrix of the standard deviation is calculated as follows:

$$\mathbf{C}_{\hat{\mathbf{X}}\hat{\mathbf{X}}}=E[(\mathbf{X}-\hat{\mathbf{X}})(\mathbf{X}-\hat{\mathbf{X}})^T]=\sigma_\rho^2\,(W^TW)^{-1} \quad (6)$$

$\sigma_{\hat{X}i}^2=C_{\hat{X}\hat{X}_{ii}}$ is the i^{th} diagonal coefficient of $\mathbf{C}_{\hat{\mathbf{X}}\hat{\mathbf{X}}}$. The relative standard deviation $\%\sigma_{\hat{X}_{ri}}$ is given by:

$$\%\sigma_{\hat{X}_{ri}}=100\,\sigma_{\hat{X}_i}\Big/\hat{X}_i \quad (7)$$

However, in practice, $\mathbf{W}$ is not deterministic. This problem can be solved by filtering the measurement matrix $\mathbf{Y}$ and the columns of the observation matrix $\mathbf{W}$ as described in [12].

IV. Medical Haptic Interface

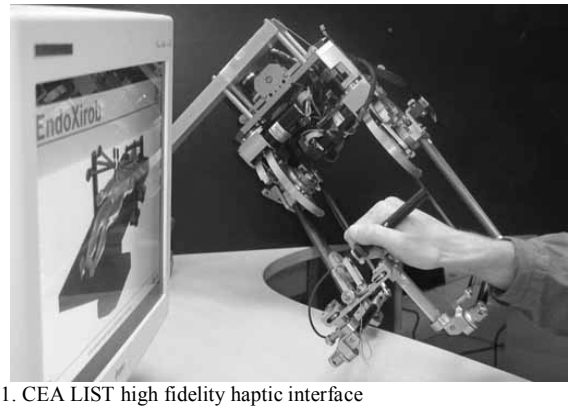

Fig. 1. CEA LIST high fidelity haptic interface

The CEA LIST has recently developed a 6DOF high fidelity haptic device for telesurgery [16]. As serial robots are quite complex to actuate (especially the distant axes of the wrist) while fully parallel robots exhibit a limited workspace, this device makes use of a redundant hybrid architecture composed of two three degrees of freedom branches connected via a platform supporting a motorized handle, having thus a total of 7 motors (Fig. 1). Moreover, extra links with constant orientation relative to the ground are introduced between the branches and the platform to reject all singularities at large orientations. This architecture is remarkably simple to implement while having a large workspace, similar to serial structures (its workspace is more than 200mm in translation in any direction and over 150° in rotation around any axis). Moreover, most of the motors which are the heaviest parts remain close to the base, thus minimizing the moving mass and increasing the transparency of the robot.

Each branch is composed of a shoulder, an arm and a forearm lever actuated by a parallelogram loop (Fig. 2). To provide a constant orientation between the support of the

handle and the shoulder (thus decoupling translational and rotational movements), a double parallelogram loop is used. Our purpose is to model and identify the serial upper branch of the interface.

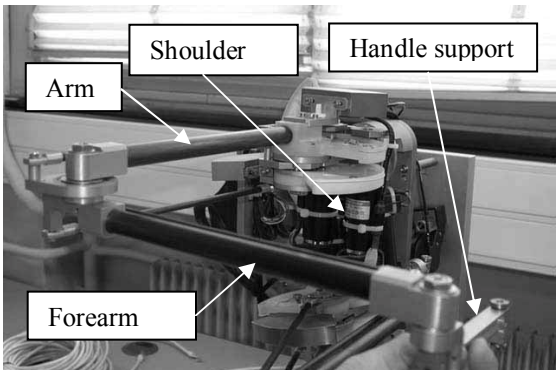

Fig. 2. Upper branch of the medical interface to be identified

V. MODELING OF THE 3DOF HAPTIC INTERFACE

A. Evaluation of the motor torques of the upper branch

In this section, the dynamic model of the upper branch is presented. Fig. 3 presents the modified Denavit Hartenberg (DHM) frames and Table 1 the DHM parameters [17].

In order to obtain an equivalent tree structure, we cut joint 7. With respect to the joint numbers defined on Fig. 3, we note for the equivalent tree structure: $\mathbf{q_a}=[q_1\ q_2\ q_5]^T$ the active joint positions vector, $\mathbf{q_p}=[q_3\ q_6\ q_4]^T$ the passive joint positions vector, $q_c=q7$ the cut joint position, $\mathbf{\Gamma_{ar}}=[\ \Gamma_{ar1}\ \Gamma_{ar2}\ \Gamma_{ar5}\ \Gamma_{ar3}\ \Gamma_{ar6}\ \Gamma_{ar4}]^T$ the joint torques vector and $\mathbf{\Gamma_m}=[\ \Gamma_1\ \Gamma_2\ \Gamma_5]^T$ the joint motorized torques.

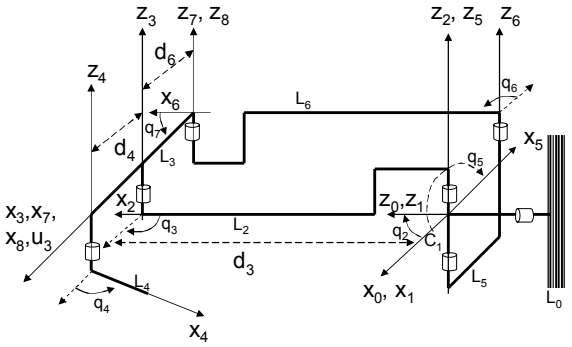

Fig. 3. DHM frames for modeling the upper branch of the medical interface

TABLE 1
DENAVIT HARTENBERG PARAMETERS

j	a(j)	μj	σj	γj	bj	αj	dj	θj	rj
1	0	1	0	0	0	0	0	q1	0
2	1	1	0	0	0	-90	0	q2	0
3	2	0	0	0	0	0	d3	q3	0
4	3	0	0	0	0	0	d4	q4	0
5	1	1	0	0	0	-90	0	q5	0
6	5	0	0	0	0	0	d6	q6	0
7	6	0	0	0	0	0	d3	q7	0
8	3	0	2	0	0	0	-d6	0	0

At present, the relations between the variables $\mathbf{q_a}$ and $\mathbf{q_p}$ are calculated. They constitute the geometric constraint equations of the closed loops, i.e. $\mathbf{q_p} = \mathbf{f_c(q_a)}$. The parallelogram loop gives linear constraint equations [15]. Since the links 2 and 6 (resp. 5 and 3) are always parallel, the (3x3) orientation matrix between frames 2 and 6 (resp. 5 and 3) is constant, that is, ${}^3\mathbf{A_5}$=constant and ${}^2\mathbf{A_6}$=constant. In our case, we obtain ${}^3\mathbf{A_5}={}^2\mathbf{A_6}=\mathbf{I_3}$ and this yields:

$$q_3=q_5-q_2 \quad \textbf{(8)}$$
$$q_6=q_2-q_5 \quad \textbf{(9)}$$

And, by writing that ${}^7\mathbf{A_8}=\mathbf{I_3}$, one obtains:

$$q_7=q_3=q_5-q_2 \quad \textbf{(10)}$$

This means that friction existing on this cut joint is seen by the third joint. The last constraint is obtained by considering the geometric constraints of the double parallelogram (Fig. 6). X_1 and (EE') are always parallel while X_4 and (EE') are always perpendicular. This yields:

$$q_4=\pi/2-q_5 \quad \textbf{(11)}$$

Knowing the constraint equations, the dynamic model of the closed loop chain is given by:

$$\mathbf{\Gamma_m}=[[\partial\mathbf{q_a}/\partial\mathbf{q_a}]^T\ [\partial\mathbf{q_p}/\partial\mathbf{q_a}]^T]\mathbf{\Gamma_{ar}}=[\mathbf{I_3}\ \mathbf{L}^T]\mathbf{\Gamma_{ar}} \quad \textbf{(12)}$$

Where $\mathbf{L}^T=[\partial\mathbf{q_p}/\partial\mathbf{q_a}]^T=\begin{bmatrix} 0 & 0 & 0 \\ -1 & 1 & 0 \\ 1 & -1 & -1 \end{bmatrix}$ and $\mathbf{\Gamma_{ar}}$ being the joint torques calculated for the equivalent tree structure.

Thus, (12) describes the dynamic model of the 3 dof branch of the medical interface. Now, the cable transmission and friction are considered.

B. Modeling of the cable transmission

The motorized joints are actuated by means of cable capstan reducers. This type of transmission is a good compromise between frictions and losses and/or slippage. Several models of cable transmissions have been designed: in [18] the transmission is considered as rigid whereas in [19] the cable flexibility is taken into account.

In this study, based on calculations and previous works on benchmarks and other haptic devices, we consider that:

- no slippage and losses occur,
- the mass of the cable is negligible and its length is practically constant,
- if the pretension of cable varies, then the Coulomb and stiction coefficients vary linearly with respect to it,
- the pretension of the cable is practically constant and can not be null.

Thus the Coulomb coefficient is constant and actuation is always possible. In our case, stiction and Coulomb coefficients are close. With these assumptions, the transmission model can be written as follows (the script d indicates that the displacements and the velocities are small):

$$\Gamma_m=K.dq_m+Bd\,\dot{q}_m+offset \quad \textbf{(13)}$$
$$\Gamma_m=[dq_m\ d\,\dot{q}_m\ 1].[K\ B\ offset]^T \quad \textbf{(14)}$$

The stiffness of the transmission can be identified by rigidly blocking the arm and the forearm, applying triangular

torques and measuring the motor position. Then we obtain an hysteretic cycle as shown in Fig. 4.

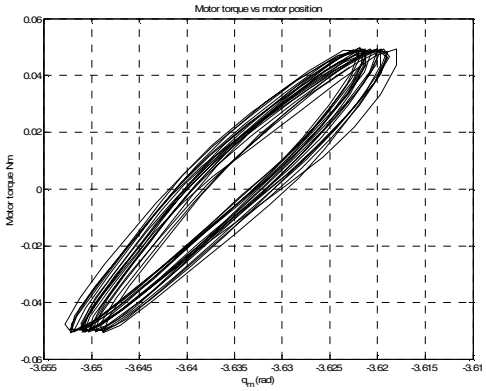

Fig. 4. Hysteretic cycle observed for each capstan transmission.

TABLE 2
STIFFNESS TRANSMISSION VALUES

Parameter	Value	Relative deviation %
K_1	2.0 Nm/rad	0.4
K_2	2.0 Nm/rad	0.3
K_5	2.0 Nm/rad	0.5

The results obtained for each capstan transmission is summed up in Table 2. Results for the damping and offset are not given as these parameters are negligible in practice.

Knowing the stiffness of the transmission, the bandwidth can be roughly evaluated taking CAD values for the inertia. In this case, the bandwidth is close to 20 Hz.

This value is well above the frequency range that will be used for the identification of the inertial parameters (0.1Hz to 2Hz). Consequently, the capstan transmission will be considered as rigid in the following sections.

C. Modeling and identification of the friction torque

The friction is in general difficult to model. Its effect is often approximated by adding viscous and Coulomb coefficients. For haptic devices, we must check that no undesirable extra nonlinear effect occurs at low velocities. This step of the modeling is essential as the haptic devices are often used at low velocities.

An attempt to identify such nonlinearities taking into account stiction has been done on a single DOF interface [20]. In this work, friction and inertia were identified together using sinusoidal velocities. However, the conditioning number of **W** (calculated using the linear regressor given by the authors) is quite high. This proves that friction coefficients are not well excited. Indeed, triangular trajectories would have been more optimal. The method described in [21] consists in measuring the motorized joint torques at different constant velocities. As practical implementation of this method, we have used triangular trajectories with various amplitudes and frequencies. QR decomposition and conditioning number of **W** had confirmed that friction coefficients are well excited.

The joint torque is calculated through current measurement. We have $\Gamma_a=NK_CI$, where Γ_a is the joint torque, N the transmission gear ratio, K_C the motor torque constant and I the current of the motor. Several types of friction have been modeled and identified in [22]. Experiences show that in our case, nonlinear effects are negligible (Fig. 5). Therefore, a classical static model (viscous and Coulomb given by equation (15)) is sufficient.

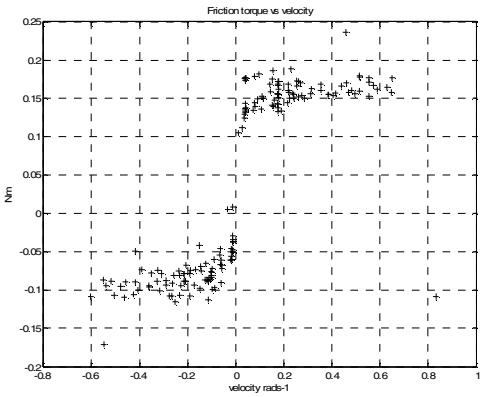

Fig. 5. Type of friction measured for each actuated joint. We can remark a dissymmetry due to offset current measurements and small gravity effect

$$\Gamma_{fi}=F_{Vi}\ \dot{q}_i+F_{Ci}\text{sign}(\dot{q}_i) \quad \textbf{(15)}$$

The results obtained with this model for the first axis are given in Table 3. However, it can not be applied directly to axes 2 and 3 as the parallelogram loop introduces couplings between their friction coefficients. By developing (12) and by keeping only the terms of friction, one obtains:

$$\Gamma_{f2}=F_{V2}\ \dot{q}_2+F_{C2}\text{sign}(\dot{q}_2)+\Gamma_{fc} \quad \textbf{(16)}$$

$$\Gamma_{f5}=F_{V5R}\ \dot{q}_5+F_{C5R}\text{sign}(\dot{q}_5)-\Gamma_{fc} \quad \textbf{(17)}$$

Where: $F_{V5R}=F_{V5}+F_{V4}$, $F_{C5R}=F_{C5}+F_{C4}$
$\Gamma_{fc}=F_{V3R}(\dot{q}_2-\dot{q}_5)+F_{C3R}\text{sign}(\dot{q}_2-\dot{q}_5)$
$F_{V3R}=F_{V3}+F_{V6}$, $F_{C3R}=F_{C3}+F_{C6}$

We recall that F_v and F_C are respectively the viscous and Coulomb friction coefficients. QR decomposition confirms that all parameters present in (16) and (17) can be identified. Notice that the friction of joint 7 is regrouped with the friction of the third joint because of (10).

In most of the cases, the friction of passive joints is smaller than those of active joints and is often neglected. In order to verify this assumption, three trajectories are designed. The first, called t1 consists in eliminating Γ_{fc} in (16) and (17) by choosing $\dot{q}_5=\dot{q}_2$. With t1, we identify $F_{V2t1}=F_{V2}$, $F_{C2t1}=F_{C2}$, $F_{V5t1}=F_{V5R}$ and $F_{C5t1}=F_{C5R}$. The second, called t2, eliminates (17) by choosing $\dot{q}_5=0$. With t2, we identify $F_{V2t2}=F_{V2}+F_{V3R}$ and $F_{C2t2}=F_{C2}+F_{C3R}$. The third, called t3 eliminates (16) by choosing $\dot{q}_2=0$. With t3, we identify $F_{V5t3}=F_{V5R}+F_{V3R}$ and $F_{C5t3}=F_{C5R}+F_{C3R}$. The results of friction identification are summed up in Table 3.

From these results, we can see that F_{V2t1} (resp. F_{V5t1}) is close to F_{V2t2} (resp. F_{V5t2}), and that F_{C2t1} (resp. F_{C5t1}) is close to F_{C2t2} (resp. F_{C5t2}). Thus friction of passive joints 3 and 6 can be neglected ($F_{V3R}=F_{V3}+F_{V6}\approx 0$, $F_{C3R}=F_{C3}+F_{C6}\approx 0$).

Moreover, we observe that the viscous coefficients have a large relative deviation. As the conditioning of **W** is close to

6 for all experiments, we can conclude that there is no significant viscous friction in the joints as in [9].

TABLE 3
IDENTIFICATION OF FRICTION TORQUES OF THE ARM

Parameter	Value	Relative deviation %
F_{V1}	0.020 Nm/(rad/s)	15.0
F_{S1}	0.130 Nm	0.9
F_{V2t1}	0.021 Nm/(rad/s)	10.0
F_{C2t1}	0.120 Nm	0.8
F_{V2t2}	0.022 Nm/(rad/s)	9.0
F_{C2t2}	0.120 Nm	0.7
F_{V5t1}	0.018 Nm/(rad/s)	20.0
F_{C5t1}	0.120 Nm	0.9
F_{V5t3}	0.020 Nm/(rad/s)	15.0
F_{V5t3}	0.120 Nm	0.9

D. Minimum inertial parameters

The minimum set of inertial parameters of the equivalent tree structure is calculated thanks to SYMORO+. The additional regroupings are the followings: $^2\mathbf{JR_2}=^2\mathbf{J_2}+^6\mathbf{J_6}$ because of (9) and $^3\mathbf{JR_3}=^3\mathbf{J_3}+^5\mathbf{J_5}$ because of (8) [15]. Because of the constant orientation between the shoulder and the handle support, inertial parameters of link 4 are regrouped with those of the first link. The minimum inertial parameters are: ZZ1R, MX1, MY1R, FV_1, FS_1, $OFFSET_1$, XX2R, XY2R, XZ2R, YZ2R, ZZ2R, MX2R, MY_2, FV2, FS_2, $OFFSET_2$, XX3R, XY3R, XZ3R, YZ3R, ZZ3R, MX3R, MY3, MX5R, MY_5, FV5R, FS5R, $OFFSET_5$ and MY_6. The script R indicates that the parameter is regrouped with other parameters.

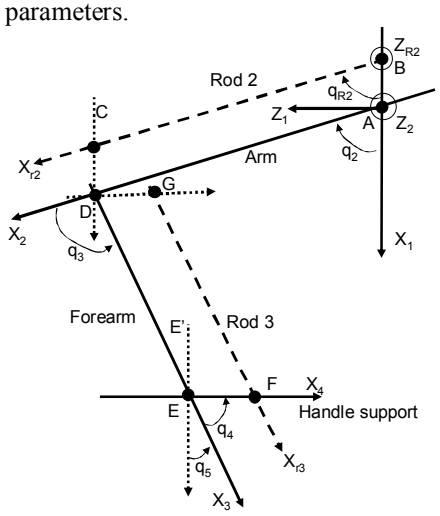

Fig. 6. Double parallelogram loop for the handle support

The double parallelogram of the handle support is not included in the modeling. This is justified by the following reasoning inspired from [15]:

- The arm and the second rod (referenced R2) have the same angular velocity, like the forearm and the third rod (referenced R3). Thus, the inertia and friction of the second (respectively third) rod can not be distinguished from those of the arm (respectively forearm). They are regrouped by: $^2\mathbf{JR'}_2=^2\mathbf{JR}_2+^{R2}\mathbf{J}_{R2}$, $^3\mathbf{JR'}_3=^3\mathbf{JR}_3+^{R3}\mathbf{J}_{R3}$ for the inertial parameters and the same for the friction.
- If the arm (resp. forearm) and the second (resp. third) rod have the same translational velocity, one obtains $MX2R'=MX2R+MX_{R2}$ and $MY2R=MY_2+MY_{R2}$ (resp. $MX3R'=MX3R+MX_{R3}$ and $MY3R=MY_3+MY_{R3}$). This means that first inertia moments of the rods and links can not be distinguished in the dynamic model and are regrouped together. Else, MYR2 (resp. MYR3) can be identified. However, in our case, these parameters prove to be negligible because the rods are light and thin.
- The parameters of the mechanical piece CDG are regrouped with those of the platform.

E. Conclusion

In this section, the modeling of the upper branch of the medical interface has been presented. The main difficulty was to model the friction. Experiences have shown that the nonlinear effects, at low velocities, are smaller than the Coulomb and viscous effects. They can be neglected. However, it appears that these parameters are sensitive to cable wear. Hence, they must be identified and modeled regularly. The double parallelogram loop is often neglected in the modeling because of the lightness and thinness of the rods. However, we have shown that one parameter per rod can be identified.

VI. IDENTIFICATION RESULTS

In this section, the identification of the set of minimum parameters is presented. "Exciting trajectories" are designed by mixing triangular and sinusoidal trajectories with various frequencies and amplitudes. Triangular positions give constant velocities and excite well gravity and friction parameters; while sinusoidal positions give sinus accelerations and excite well inertia parameters. Appropriate data treatment was designed as in [12] and [13]. **W** is a (15000x16) matrix. The identified values of parameters are summed up in Table 4. The conditioning number of **W** is close to 50. The trajectories are thus enough exciting for identifying the inertial parameters [12].

TABLE 4
INERTIAL PARAMETERS ESTIMATION

Parameter	Value	Relative deviation %
ZZ1R	0.0510 Kgm^2	0.4480
MY1R	-0.0260 Kgm	1.200
FV1	0,023 Nm/(rad/s)	22.000
FS1	0.1179 Nm	0.7823
XX2R	-0.0209 Kgm^2	0.8488
ZZ2R	0.0295 Kgm^2	0.3538
MX2R	-0.0225 Kgm	0.7660
FV2R	0,032 Nm/(rad/s)	21.000
FS2	0.1240 Nm	0.8120
OFFSET2	0.0200 Nm	3.3470
XX3R	-0.0110 Kgm^2	1.2500
ZZ3R	0.0130 Kgm^2	0.4320
MX3R	-0.0310 Kgm	0.4130
FV5R	0,031 Nm/(rad/s)	20.000
FS5R	0.1152 Nm	1.2580
OFFSET5	0.0300 Nm	1.100

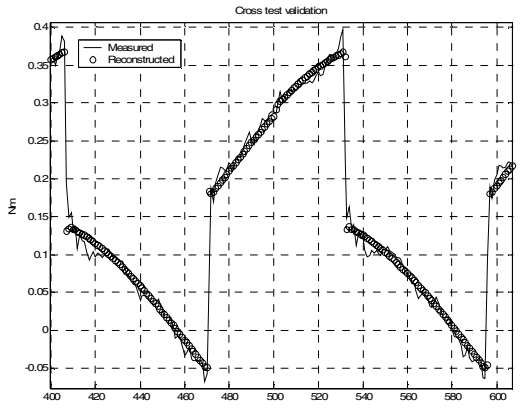

Fig. 7: Cross test validation, compares the measured and estimated torques applied to the forearm

Parameters MX1R, OFFSET1, MY2R, MY3R, MX5R, MY5, MY6 and nondiagonal components of inertia tensor are missing because they are small or have small influence compared with the others. We checked that when identified they have a large relative deviation, and that when removed from the identification model, the estimation of the other parameters is not perturbed. We checked also that identified values are compatible with those obtained from CAD.

Cross tests validations have been performed. They consist in comparing the experimental data obtained along a trajectory not used during the identification procedure and data reconstructed from the identified parameters. Results obtained for the forearm (given in Fig. 7) show that the estimated torque follows the measured torque closely.

VII. PERFORMANCES OF THE UPPER BRANCH

Knowing the values of the minimum inertial parameters, it is possible to calculate the apparent mass, operational friction and stiffness felt by the operator. This characterizes the distortion introduced by the haptic interface. In the operational space, the model of the 3 dof haptic device can be written as following:

$$\mathbf{F_{op}}=\mathbf{M_{op}}.\ddot{\mathbf{X}}+\mathbf{B_{op}}.\dot{\mathbf{X}}+\mathbf{K_{op}}.\mathbf{X}+\mathbf{F_{cop}}.\mathbf{sign}(\dot{\mathbf{X}})+\mathbf{F_d} \quad (18)$$

Where $\mathbf{F_{op}}$ is the force applied by the operator, $\mathbf{X}$, $\dot{\mathbf{X}}$ and $\ddot{\mathbf{X}}$ are respectively the position, velocity and acceleration vector in the operational space, $\mathbf{M_{op}}$ is the (3x3) apparent mass matrix defined by $\mathbf{M_{op}}=\mathbf{J^{-T}A(q)J^{-1}}$, ($\mathbf{J}$ is the (3x3) jacobian matrix equals to $\mathbf{J}=\partial f(q)/\partial q$), $\mathbf{B_{op}}$ is the apparent viscous friction matrix which equals to $\mathbf{B_{op}}=\mathbf{J^{-T}F_VJ^{-1}}$, $\mathbf{K_{op}}$ is the operational stiffness matrix given by $\mathbf{K_{op}}=\mathbf{J^{-T}K_{tot}J^{-1}}$ and $\mathbf{F_{cop}}=\mathbf{J^{-T}F_c}$ is the operational Coulomb friction matrix. For calculating $\mathbf{K_{tot}}$, we do not include the structural flexibility. This yields:

$$K_{tot}=1/(1/K_T+1/K_E) \quad (19)$$

where K_T is the transmission stiffness identified in section 4 and K_E the electric stiffness which equals 2Nm/rad.

$\mathbf{F_d}$ given by (20), is the torque neglected in the linear characterization of operational dynamics of the interface. The greater the velocity and angular range, the higher the disturbance will be.

$$\mathbf{F_d}=\mathbf{J^{-T}}(\mathbf{Q(q)}+\mathbf{C(q,\dot{q})\dot{q}}-\mathbf{A(q)\dot{J}\dot{q}}) \quad (20)$$

The apparent mass and the operational stiffness and friction, felt by the operator, can be calculated at all configurations in the workspace. For instance, Fig. 8 shows the maximum values of the diagonal components (called respectively Mxx, Myy and Mzz) obtained through SVD decomposition of the apparent mass matrix, and shows the values of the diagonal components of the stiffness matrix (called respectively Kxx, Kyy and Kzz).

The variation of the maximum values of Coulomb friction, calculated through SVD decomposition, and diagonal components of the operational viscous friction matrix, are illustrated Fig. 9. They have been calculated around a natural position for the operator.

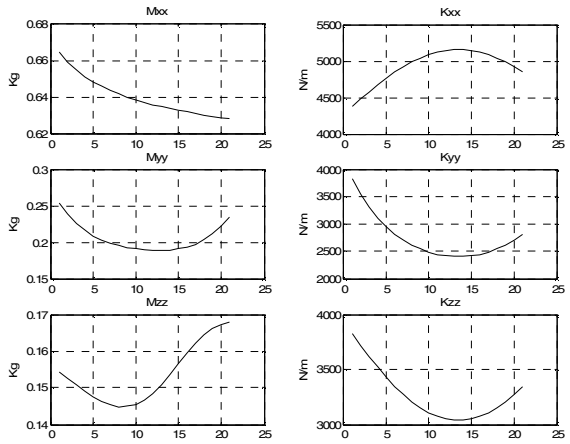

Fig. 8. Apparent mass and operational stiffness around a natural position

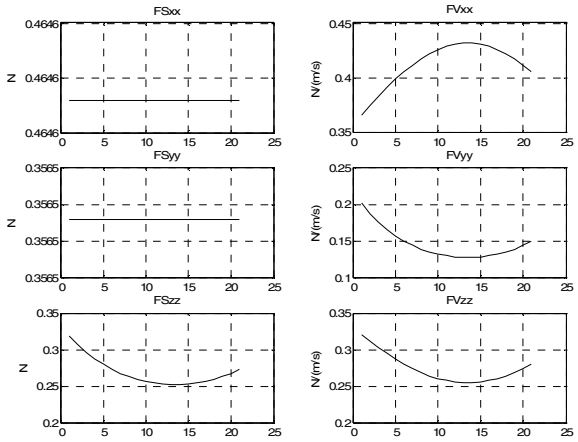

Fig. 9. Coulomb and viscous operational friction around a natural position

The maximum weight felt by the operator is close to 650g. This value is mainly due to the masses of the extremities of the links of the structure. Due to limited reduction ratios, the apparent mass resulting from the inertia of the rotors of the motors is limited, as well as the apparent mass of the counter-weights which are compensating the gravity effect in the parallelogram. Although their masses are close to 1Kg, their inertial effect is limited due to their proximity with the rotation axes. For others positions in the operational space, the maximum value can reach 800g.

The stiffness varies between 2000 N/m and 5000 N/m. That means the electric and transmission stiffness do not

affect the haptic rendering. The cable transmission is well designed. However, these values can be defined as a maximum bound. Indeed, the structural flexibility is not included, and if too high, it can affect the haptic rendering. Notice that it is usually neglected.

The maximum values of operational dry friction vary between 0.3N and 0.4N. This is equivalent to move a mass of 30g or 40g. We can admit that dry friction affects weakly the haptic rendering.

The gravity effect can be compensated by means of a predictive control. Indeed, the gravity parameters are stable and, in this case, the gravity model is quite "simple". But, the compensation of friction is more difficult because of its sensitivity to noises and cable wear. A solution consists in implanting underestimated friction coefficients as in [23]. In our case, this strategy of control is implemented.

VIII. Conclusion and Future Works

Experimental results given along this paper show that it is possible to apply an identification method using inverse model and least squares method frequently used for industrial robots to identify dynamic parameters of haptic devices, which present a completely different behavior (lower friction, lower mass). Associated with a proper parametric model, these values can be used to evaluate the distortion introduced by the haptic device. It is thus possible to assess the qualities and drawbacks of the interface and to improve its design. It is also possible to compensate adverse effects by appropriate control laws.

One important aspect of the proposed methodology is that no specific assumption is made. Therefore, the protocol exhibited along this paper can be applied to any haptic devices. It can be used for comparing performances between several interfaces or different types of transmission. However, this identification method needs position and current measurements. In order to get reliable results, especially for friction torque, an accurate current measurement is needed. In addition, the identification was made under the rigid modeling hypothesis.

Future works concern the use of this method to identify the 6 dof medical interface. The structural flexibility will be also identified in order to determinate its influence in the haptic rendering. Several techniques of identification of localized flexibilities have been designed and tested in [24] and could be extended to multi degrees of freedom model including transmission and structural stiffness.

References

[1] P.A. Millman, M. Stanley and JE. Colgate, "Design of a high performance haptic interface to virtual environments", *Proc. IEEE Annual Virtual Reality Symposium*, 1993, p. 216-222

[2] J.J. Abbot and A.M. Okamura, "A sufficient condition for passive virtual walls with quantization effects", *Proc. IMECE 2004*, USA, p. 1065-1073

[3] J. Colgate and G. Schenkel, "Passivity of a class of sampled data systems: application to haptic interfaces", *American Control Conference*, Baltimore 1994, p. 3236-3240

[4] N. Diolaitti, G. Niemayer, F. Barbagli and J. Kenneth Salisbury, "A criterion for the passivity of haptic devices", *Proc. IEEE Int. Conf. on Robotics and Automation*, 2005, p. 2463-2468

[5] M. Moreyra and B. Hannaford, "A practical measure of dynamic response of haptic devices", *Proc. IEEE Int. Conf. on Robotics and Automation*, Leuven, 1998, p.369-374

[6] A. Frisoli and M. Bergamasco, "Experimental identification and evaluation of performance of a 2 dof haptic display", *Proc. IEEE Int. Conf. on Robotics and Automation*, 2003, p. 3260-3265

[7] C.D. Lee, D.A. Lawrence and L.Y. Pao, "Dynamic modeling and parameter identification of a parallel haptic interface", *Proc. 10th Symp. Haptic Interfaces for Virtual Environments and Teleoperator Systems, IEEE Virtual Reality Conf.*, Orlando, 2002, p. 172-179

[8] A.M. Tahmasebi, B. Taati, F. Mobasser and K. Hashtrudi-Zaad, "Dynamic parameter identification and analysis of a PHANToM™ haptic device", *Proc. IEEE Conf. on Control Applications*, Toronto, August 2005, pp. 1251-1256

[9] M. C. Cavusoglu and D. Feygin, "A critical study of the mechanical and electrical properties of PHANToM haptic interface and improvements for high performance control", *Presence: Teleoperators and Virtual Environments*, 2002

[10] M. Gautier and W. Khalil, "Direct calculation of minimum set of inertial parameters of serial robots", *IEEE Transactions on Robotics and Automation*, Vol. 6(3), June 1990

[11] M. Gautier, W. Khalil and P. P. Restrepo, "Identification of the dynamic parameters of a closed loop robot", *Proc. IEEE on Int. Conf. on Robotics and Automation*, Nagoya, may 1995, p. 3045-3050

[12] M. Gautier, "Dynamic identification of robots with power model", *Proc. IEEE Int. Conf. on Robotics and Automation*, Albuquerque, 1997, p. 1922-1927

[13] F. Khatounian et al., "Parameter identification of a single degree of freedom haptic interface", *14th IFAC Symp. on System Identification, SYSID 2006*, Newcastle, Australia, 2006, p. 249-254

[14] M. Gautier , "Numerical calculation of the base inertial parameters", *Journal of Robotics Systems*, Vol. 8, august 1991, p. 485-506

[15] F. Bennis and W. Khalil, "Minimum inertial parameters of robots with parallelogram closed loop", *IEEE Trans. On Systems, Man and Cybernetics*, Vol. SMC 21, 1991, p., 318-326

[16] F. Gosselin, C. Bidard, J. Brisset, "Design of a high fidelity haptic device for telesurgery", *IEEE Int. Conf. on Robotics and Automation*, Barcelone 2005, p. 206-211

[17] W. Khalil and J.F. Kleinfinger, "A new geometric notation for open and closed loop robots", In: *IEEE Int. Conf. On Robotics and Automation*, San Francisco USA, April 1986, pp. 1147-1180

[18] J.J. Lee, "Tendon driven manipulator: analysis, synthesis and control", Ph. D. dissertation, Harvard university, 1991

[19] Y.H. Lee and J.J. Lee, " Modeling of the dynamics of the tendon driven robotic mechanisms with flexible tendons", *Mechanism and Theory Vol. 38*, march 2003, p. 1431-1447

[20] C. Richard, M.R. Cutkosky and K. MacLeon, "Friction identification for haptic display", *Proc. ASME IMECE*, Nashville, November 1999, p. 327-334

[21] R. Specht, and R. Isermann, "On-line identification of inertia, friction and gravitational forces applied to an industrial robot", *Proc. IFAC Symp. on Robot Control, SYROCO'88*, 1988, p. 88.1-88.6

[22] B. Armstrong, "Stick slip and control in low speed motion", *IEEE Transactions on Automatic Control Vol. 38(10)*, October 1993, p. 1483-1496

[23] M. Mahvash and A.M. Okumura, "Friction compensation for a force feedback telerobotic system", *Proc. IEEE on Int. Conf. on Robotics and Automation*, Orlando, May 2006, p. 3268-3273

[24] M.T. Pham, M. Gautier and P. Poignet "Identification of joint stiffness with band pass filtering", *Proc. IEEE on Int. Conf. on Robotics and Automation*, Seoul, may 2001, p. 2867-2872